

**NASA CONTRACTOR
REPORT**



N73-33847
NASA CR-2345

NASA CR-2345

CASE FILE
COPY FILE

**THE DEVELOPMENT OF A PSEUDO-NYQUIST
ANALYSIS TECHNIQUE FOR HYBRID
SAMPLED-DATA CONTROL SYSTEMS**

by Milford G. Burnitt and Charles W. Davis

Prepared by

CHRYSLER CORPORATION

SPACE DIVISION

New Orleans, La. 70189

for George C. Marshall Space Flight Center

1. REPORT NO. NASA CR-2345		2. GOVERNMENT ACCESSION NO.		3. RECIPIENT'S CATALOG NO.	
4. TITLE AND SUBTITLE THE DEVELOPMENT OF A PSEUDO-NYQUIST ANALYSIS TECHNIQUE FOR HYBRID SAMPLED-DATA CONTROL SYSTEMS				5. REPORT DATE October 1973	
				6. PERFORMING ORGANIZATION CODE M220	
7. AUTHOR(S) Milford G. Burnitt and Charles W. Davis				8. PERFORMING ORGANIZATION REPORT #	
9. PERFORMING ORGANIZATION NAME AND ADDRESS Chrysler Corporation Space Division Michoud Assembly Facility New Orleans, La. 70189				10. WORK UNIT NO.	
				11. CONTRACT OR GRANT NO. NAS 8-4016	
				13. TYPE OF REPORT & PERIOD COVERED Low Series Contractor <u>Topical</u>	
12. SPONSORING AGENCY NAME AND ADDRESS National Aeronautics and Space Administration Washington, D. C. 20546				14. SPONSORING AGENCY CODE	
15. SUPPLEMENTARY NOTES					
16. ABSTRACT The stability characteristics of a launch vehicle, as a function of gain and phase variations at the thrust vector controller (TVC), cannot be obtained using classical sampled-data control theory if the launch vehicle attitude control system contains both sampled-data and continuous feedback control loops. A method has been developed which can be used to generate a sampled-data pseudo-Nyquist plot for gain and phase variations at the controller. This method was developed and used to determine the stability characteristics of the Saturn IB launch vehicle in the backup guidance mode.					
17. KEY WORDS			18. DISTRIBUTION STATEMENT		
19. SECURITY CLASSIF. (of this report) Unclassified		20. SECURITY CLASSIF. (of this page) Unclassified		21. NO. OF PAGES 41	22. PRICE Domestic, \$3.00 Foreign, \$5.50

TABLE OF CONTENTS

	Page
INTRODUCTION	1
1.0 STATEMENT OF THE PROBLEM	2
2.0 DEVELOPMENT OF SOLUTION TECHNIQUE	4
3.0 APPLICATION OF SOLUTION TECHNIQUE TO SATURN IB CONTROL SYSTEM IN THE BACKUP GUIDANCE MODE	9
4.0 COMPUTER SIMULATION VERIFICATION OF STABILITY RESULTS	14
CONCLUDING REMARKS	21
APPENDIX A	A-1
APPENDIX B	B-1
REFERENCES	R-1

LIST OF ILLUSTRATIONS

<u>Figure</u>	<u>Title</u>	<u>Page</u>
1	SATURN IB FIRST-STAGE PITCH/YAW ATTITUDE CONTROL SYSTEM	2
2	SIMPLIFIED BLOCK DIAGRAM FOR SATURN IB FIRST-STAGE PITCH/YAW ATTITUDE CONTROL SYSTEM	3
3	TYPICAL NYQUIST PLOT FOR OPEN LOOP AT TVC FOR THE SATURN IB FIRST-STAGE PITCH/YAW ATTITUDE CONTROL SYSTEM IN THE PRIMARY GUIDANCE MODE	6
4	PSEUDO-NYQUIST PLOT FOR THE SATURN IB FIRST-STAGE PITCH/YAW ATTITUDE CONTROL SYSTEM IN THE BACKUP GUIDANCE MODE	11
5	CONFIRMATION OF LOW-FREQUENCY GAIN MARGINS FROM PSEUDO-NYQUIST PLOT	16
6	PSEUDO-NYQUIST PLOT USING MODIFIED FIRST BENDING GENERALIZED MASS	17
7	PSEUDO-NYQUIST PLOT USING MODIFIED SECOND BENDING GENERALIZED MASS	18
8	CONFIRMATION OF FIRST BENDING MODE STABILITY MARGINS FROM PSEUDO-NYQUIST PLOT	19
9	CONFIRMATION OF SECOND BENDING MODE STABILITY MARGINS FROM PSEUDO-NYQUIST PLOT	19

LIST OF TABLES

<u>Table</u>		<u>Page</u>
1	MULTIVALUED SOLUTIONS AT LOW-FREQUENCY GAIN AND PHASE MARGIN CROSSOVER FREQUENCIES	10
2	REFLECTED BENDING MODE OPEN AT TVC PHASE AND GAIN CHARACTERISTICS	14

LIST OF SYMBOLS

A_R	REFERENCE AREA (m^2)
a_o	ATTITUDE ERROR CONTROL GAIN (deg per deg)
a_1	ATTITUDE RATE CONTROL GAIN (deg per deg/sec)
$C_{n\alpha}$	NORMAL FORCE COEFFICIENT GRADIENT (per radian)
F	TOTAL AXIAL THRUST (Newtons)
F_G	TOTAL GIMBAL THRUST (Newtons)
$F_{\phi}(s)$	ATTITUDE ERROR SHAPING NETWORK TRANSFER FUNCTION
$F_{\dot{\phi}}(s)$	ATTITUDE RATE SHAPING NETWORK TRANSFER FUNCTION
$F_{\dot{\gamma}}(s)$	ACCELEROMETER SHAPING NETWORK TRANSFER FUNCTION
$G_{TVC}(s)$	ACTUATOR TRANSFER FUNCTION
G_{ZOH}	ZERO-ORDER-HOLD TRANSFER FUNCTION
g_2	ACCELEROMETER CONTROL GAIN (DEG PER M/SEC ²)
\bar{g}	AXIAL ACCELERATION (m/sec^2)
I	PITCH INERTIA ABOUT CENTER OF MASS ($kg-m^2$)
j	COMPLEX OPERATOR
M	TOTAL VEHICLE MASS (Kg)
M_{Bi}	GENERALIZED MASS OF THE i th BENDING MODE (Kg)
$N_{\phi}(s)$	NUMERATOR POLYNOMIAL FOR SENSED PITCH ATTITUDE ERROR TO ENGINE GIMBAL ANGLE TRANSFER FUNCTION
$N_{\dot{\phi}}(s)$	NUMERATOR POLYNOMIAL FOR SENSED PITCH ATTITUDE RATE TO ENGINE GIMBAL ANGLE TRANSFER FUNCTION
$N_{\dot{\gamma}}(s)$	NUMERATOR POLYNOMIAL FOR SENSED LATERAL ACCELERATION TO ENGINE GIMBAL ANGLE TRANSFER FUNCTION

LIST OF SYMBOLS (Continued)

P(S)	DENOMINATOR POLYNOMIAL FOR SENSED CONTROL SIGNALS TO ENGINE GIMBAL ANGLE TRANSFER FUNCTIONS
q	DYNAMIC PRESSURE (N/m^2)
S_E	FIRST MASS MOMENT OF THE GIMBAL ENGINES (Kg-m)
T	FLIGHT TIME (seconds)
T_s	SAMPLING PERIOD (seconds)
V	RELATIVE VELOCITY (m/sec)
X	TOTAL LONGITUDINAL DRAG (Newtons)
\bar{X}_A	DISTANCE FROM CENTER OF GRAVITY TO ACCELEROMETER LOCATION-POSITIVE AFT (m)
X_{cp}	CENTER OF PRESSURE LOCATION FORWARD OF GIMBAL POINT (m)
X_E	CENTER OF GRAVITY LOCATION FORWARD OF GIMBAL POINT (m)
Y	LATERAL DISPLACEMENT PERPENDICULAR TO TRAJECTORY (m)
$Y_i(A)$	DISPLACEMENT OF THE i th BENDING MODE AT THE ACCELEROMETER LOCATION
$Y_i'(A)$	ROTATION OF THE i th BENDING MODE AT THE ACCELEROMETER LOCATION (per m)
$Y_i'(PG)$	ROTATION OF THE i th BENDING MODE AT THE PLATFORM LOCATION (per m)
$Y_i'(RG)$	ROTATION OF THE i th BENDING MODE AT THE RATE GYRO LOCATION (per m)
$Y_i(XE)$	DISPLACEMENT OF THE i th BENDING MODE AT THE GIMBAL POINT
$Y_i'(XE)$	ROTATION OF THE i th BENDING MODE AT THE GIMBAL POINT (per m)

LIST OF SYMBOLS (Continued)

β_C	COMMANDED ENGINE GIMBAL ANGLE (RADIAN)
β_E	ENGINE GIMBAL ANGLE (Radians)
\dot{y}_s	SENSED LATERAL ACCELERATION OF VEHICLE (m/sec ²)
ζ_{B_i}	DAMPING RATIO OF <i>i</i> th BENDING MODE
η_i	GENERALIZED COORDINATE OF THE <i>i</i> th BENDING MODE (m)
θ_E	MOMENT OF INERTIA OF GIMBAL ENGINES (Kg-m ²)
ϕ	PITCH ATTITUDE (Radians)
ϕ_s	SENSED PITCH ATTITUDE ERROR (Radians)
$\dot{\phi}_s$	SENSED PITCH ATTITUDE RATE (Rad/sec)
ω	FREQUENCY (Rad/sec)
ω_{B_i}	FREQUENCY OF THE <i>i</i> th BENDING MODE (Rad/sec)
ω_s	SAMPLING FREQUENCY (Rad/sec)

SUMMARY

The stability characteristics of a launch vehicle as a function of gain and phase variations at the thrust vector controller (TVC), cannot be obtained using classical sampled-data control theory if the launch vehicle attitude control system contains both sampled-data and continuous feedback control loops. This poses a unique problem for the analyst in determining the stability characteristics of the vehicle, because the control system design criteria are generally stated in terms of gain and phase variations at the controller. In order to fill this void in the analysis and design techniques of sampled-data systems with both sampled-data and continuous feedback control loops, a method is described which can be used to generate a pseudo-Nyquist plot for measuring gain and phase variations at the controller. The pseudo-Nyquist plot can be used to assess the stability characteristics of the vehicle in terms of the design criteria. This method was developed and used to determine the stability characteristics of the Saturn IB launch vehicle in the backup guidance mode. The validity of the method is established by correlating the frequency response results from the new method with the time response results from a computer simulation.

INTRODUCTION

The first-stage pitch/yaw attitude control system for the Saturn IB launch vehicle consists of attitude error, attitude rate, and accelerometer control loops. The attitude rate and accelerometer control loops process continuous analog signals while the attitude error control loop processes a discrete signal which is updated every 0.04 seconds (25 samples per second). Early Saturn IB studies verified that the high-frequency attitude error sampling had little effect on the stability and response characteristics of the vehicle; consequently, the vast majority of the work performed on the Saturn IB control system ignored the attitude error sampling effects and treated the attitude error loop as a continuous, nonsampled feedback loop. This permitted stability analyses of the system using classical control theory for continuous feedback systems. During the course of the Apollo program, a backup guidance system was adopted for the Saturn IB and Saturn V vehicles. The backup guidance system utilizes the attitude error signal computed in the spacecraft computer for display to the Astronauts. This attitude error signal is updated at a variable sample rate with a predominant sampling period of 0.5 second (2 samples per second). At this low sampling frequency, the sampled-data effects of the attitude error signal cannot be ignored in analyzing the stability and response characteristics of the Saturn IB vehicle in the backup guidance mode. To evaluate the stability characteristics of this system, sampled-data analysis techniques are required.

Stability analyses of the Saturn IB control system in the backup guidance mode present an analysis problem which has been encountered in previous studies (references 1 and 2) of launch vehicles with sampled-data control systems. The analysis problem is one of obtaining an explicit solution for the frequency response of the system in terms of gain and phase variations at the thrust vector controller (TVC) (actuator) for a control system with both sampled-data and continuous feedback loops. A solution to this problem is vital because the control system design criteria are generally stated in terms of gain and phase variations at the controller. Up to now, applications of conventional analysis techniques to sampled-data control systems, including the Saturn IB control system in the backup guidance mode, have yielded only frequency response information in terms of gain and phase variations in the sampled control loop. Earlier attempts (references 1 and 2) to obtain information about gain and phase variations at the actuator resulted in approximate techniques which were valid only for a restricted range of sampling periods. These approximate techniques are not applicable to the Saturn IB control system in the backup guidance mode because of the extremely slow sampling rates of the attitude error loop (e.g., 1 to 3 samples per second).

This report presents a method for determining the open loop phase and gain characteristics at the input to the TVC of a control system with both sampled-data and continuous feedback control loops. The difficulties associated with analyzing this type of system are described in section 1.0, and the analysis technique developed to circumvent these difficulties is presented in section 2.0. The pseudo-Nyquist plot is introduced in section 2.0 as an aid for interpreting the results of the method. An example problem is presented in section 3.0, illustrating the application of the new technique and the pseudo-Nyquist plot in evaluating the stability of the Saturn IB pitch/yaw attitude control system in the backup guidance mode. The open loop gain and phase characteristics at the TVC, predicted by the new analysis technique, are verified in section 4.0 by correlating the frequency response results from the pseudo-Nyquist plot with the time response results from a computer simulation.

1.0 STATEMENT OF THE PROBLEM

A simplified block diagram of the Saturn IB first stage flight control system is shown in figure 1. This sampled-data control system is comprised of two continuous feedback loops and one sampled-data feedback loop. This type of sampled-data control system presents a unique problem because classical sampled-data analysis techniques cannot be used directly to determine the system stability margins in terms of gain and phase variations at the input to the TVC. The parameter K in figure 1 is a complex gain factor which has been introduced for the purpose of measuring the gain and phase margins of the system at the input to the TVC. The nominal value of K is $1.0 \angle 0.0^\circ$.

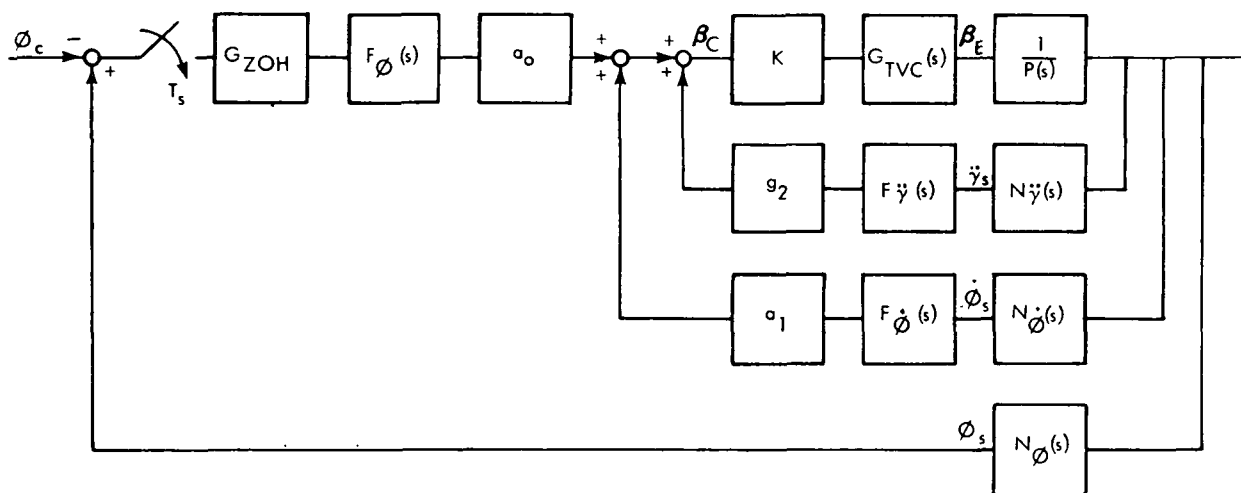


Figure 1. Saturn IB First-Stage Pitch/Yaw Attitude Control System

In order to obtain information about the gain and phase variations at the input to the TVC in figure 1, the parameter K must appear exclusively in the numerator of the open loop transfer function. For instance, if it is assumed that the control system in figure 1 is completely continuous (i.e. ignoring the sample and hold element); then from superposition, the open loop transfer function of the system open at TVC (OPTVC (s) in shorthand notation) is

$$\text{OPTVC}(s) = \frac{K a_0 G_{\text{TVC}}(s) F_{\phi}(s) N_{\phi}(s)}{P(s)} - \frac{K a_1 G_{\text{TVC}}(s) F_{\dot{\phi}}(s) N_{\dot{\phi}}(s)}{P(s)} - \frac{K g_2 G_{\text{TVC}}(s) F_{\ddot{\phi}}(s) N_{\ddot{\phi}}(s)}{P(s)} \quad (1)$$

In equation (1), K appears in all three terms of the open loop transfer function; therefore, K can be used to measure the stability margins or the allowable variations in the system characteristics (e.g. tolerances) at this point in the control system.

No open-at-TVC transfer function exists for the sampled-data system given in figure 1, because the pulse-data transfer function of the system must be taken at the sampler. To obtain this transfer function, it is convenient to reduce the block diagram of figure 1 to the one in figure 2.

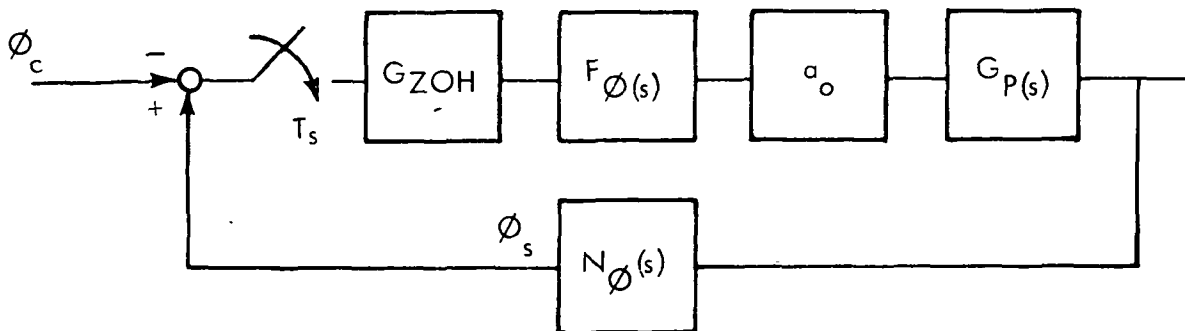


Figure 2. Simplified Block Diagram for Saturn IB First-Stage Pitch/Yaw Attitude Control System

The $G_p(s)$ transfer function in figure 2, which combines the rate and normal acceleration feedback loops with the plant and K, is given by

$$G_p(s) = \frac{K G_{TVC}(s)}{P(s) - K G_{TVC}(s) \left(g_2 \bar{F}_j(s) N_j(s) + a_1 F_\phi(s) N_\phi(s) \right)} \quad (2)$$

The pulsed-data transfer function of the system open at the sampler in figure 2 is simply

$$OPAO(s)^* = \left(-a_0 G_{ZOH}(s) F_\phi(s) N_\phi(s) G_p(s) \right)^* \quad (3)$$

Substituting for $G_p(s)$ in equation (3), the result in more general terms is

$$OPAO(s)^* = \left(\frac{-a_0 K G_{ZOH}(s) F_\phi(s) N_\phi(s) G_{TVC}(s)}{P(s) - K G_{TVC}(s) \left(g_2 \bar{F}_j(s) N_j(s) + a_1 F_\phi(s) N_\phi(s) \right)} \right)^* \quad (4)$$

The only stability information that can be directly obtained from equation (4) is the absolute stability of the system and the effect of variations in the attitude error channel. No stability information about variations in the attitude rate channel, variations in the normal acceleration channel, or variations at the input to the TVC can be directly obtained from equation (4). An iterative method can be used to determine the gain margin of the system at the input to the TVC. For example, a family of Nyquist plots can be obtained as a function of K using equation (4). The value of K that causes the Nyquist plot to pass through $1.0/180^\circ$ is the gain margin of the system. This iterative method is cumbersome and does not provide a coherent picture of the overall system stability characteristics as a function of K. Herein lies the problem: Current sampled-data control theory does not give an explicit solution for obtaining stability information about gain and phase variations in the attitude rate channel, normal acceleration channel, or at the input to the TVC for the Saturn IB attitude control system in the backup guidance mode. Therefore, a new analysis technique is needed which yields stability information about gain and phase characteristics at the input to the TVC or at other points of interest in the system. CCSD has developed such a technique. The new technique and the pseudo-Nyquist plot, introduced to interpret the multivalued solutions from the new technique, are described in the next section.

2.0 DEVELOPMENT OF SOLUTION TECHNIQUE

2.1 Inverse Function Concept

The analysis approach generally taken in computing an open-at-TVC Nyquist plot for the primary Saturn IB attitude control system (continuous system), is to substitute values of $s = j\omega$, and $K = 1.0/0^\circ$ into equation (1) and compute the

open-at-TVC gain and phase characteristics. At a particular frequency ($\omega = \omega_1$), the open loop gain and phase computed from equation (1) is:

$$\text{OPTVC}(j\omega_1) = A_1/\theta_1 = \frac{-a_0 G_{\text{TVC}}(j\omega_1) F_\theta(j\omega_1) N_\theta(j\omega_1)}{P(j\omega_1)} \quad (5)$$

$$- \frac{a_1 G_{\text{TVC}}(j\omega_1) F_\theta(j\omega_1) N_\theta(j\omega_1)}{P(j\omega_1)} - \frac{g_2 G_{\text{TVC}}(j\omega_1) F_z(j\omega_1) N_z(j\omega_1)}{P(j\omega_1)}$$

The gain and phase characteristics of OPTVC ($j\omega$) are plotted as a function of frequency to obtain an open at TVC Nyquist plot. A typical open at TVC Nyquist plot for the Saturn IB first-stage pitch/yaw attitude control system in the primary guidance mode is shown in figure 3. At any given frequency on the Nyquist plot ($\omega = \omega_1$), the gain and phase changes (K) at the TVC (actuator) which will result in neutral stability (i.e., -1 on the Nyquist plot) can be obtained from equation (6).

$$K(j\omega_1) \text{OPTVC}(j\omega_1) = -1.0 \quad (6)$$

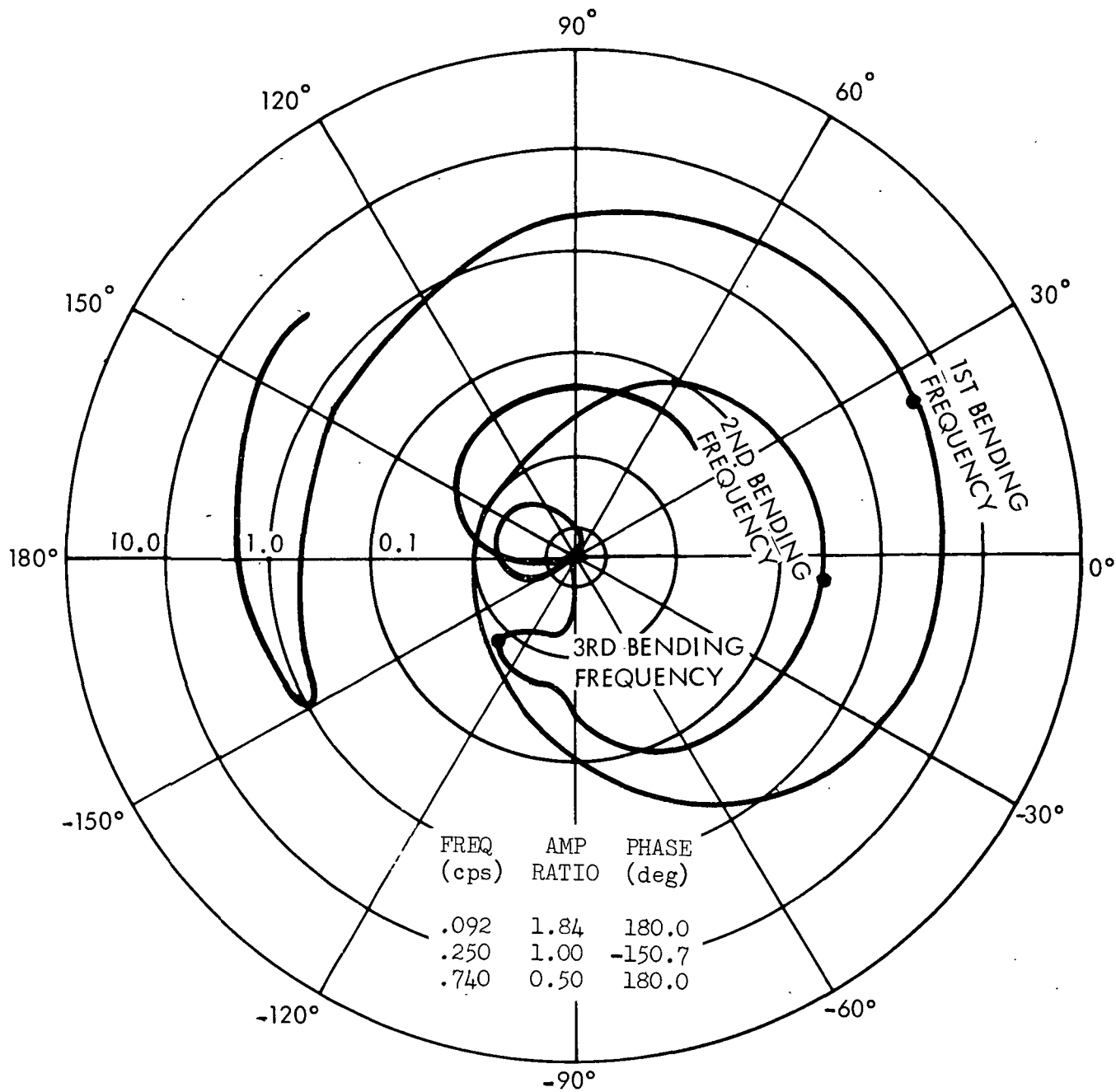
Solving equation (6) for $K(j\omega_1)$ yields:

$$K(j\omega_1) = \frac{-1.0}{\text{OPTVC}(j\omega_1)} \quad (7)$$

Thus, equation (7) shows that $K(j\omega)$ is the inverse function of the open-at-TVC frequency response. Furthermore, the complex parameter $K(j\omega)$ is an indicator of the general stability of the system relative to the -1.0 point on the Nyquist plot. For the special cases where the OPTVC ($j\omega$) frequency response crosses the unit circle and the 180-degree axis, $K(j\omega)$ corresponds to the familiar phase and gain margins defined from standard frequency response techniques (references 3, 4 and 5). Normally, the computation of $K(j\omega)$ as a continuous function of ω is not necessary in the analysis of continuous systems, because the value of $K(j\omega)$ at the frequencies of interest (e.g. unit circle crossovers and bending mode frequencies) is easily obtained by inspection from the open-at-TVC Nyquist plot.

2.2 Solution Technique

As discussed in section 1.0, there is no direct solution for the open-at-TVC frequency response of the system in figure 1 if there are both discrete and continuous feedback loops. However, there is an indirect solution to this problem utilizing the inverse function concept and the characteristic equation of the system in figure 2.



MODE	NATURAL FREQUENCY (CPS)	AMPLITUDE RATIO	PHASE (DEG)
1	.1326+01	.5061+01	24.65
2	.2327+01	.2710+00	-8.97
3	.2623+01	.1681-01	-127.39
4	.4924+01	.5909-02	170.02
5	.8532+01	.5245-01	78.10

Figure 3. Typical Nyquist Plot for Open Loop at TVC for the Saturn IB First-Stage Pitch/Yaw Attitude Control System in the Primary Guidance Mode

To simplify the notation, the following definitions are made:

$$N(s) \triangleq - \frac{a_0 G_{TVC}(s) F_{\phi}(s) N_{\phi}(s)}{P(s)} \quad (8)$$

$$D(s) \triangleq - \frac{a_1 G_{TVC}(s) F_{\phi}(s) N_{\phi}(s)}{P(s)} - \frac{g_2 G_{TVC}(s) F_j(s) N_j(s)}{P(s)} \quad (9)$$

$$Z \triangleq \frac{1}{K} \quad (10)$$

Using equations 8, 9 and 10, the pulse-transform of the characteristic equation of the system in figure 2 is:

$$1 + \left(\frac{N(s) G_{ZOH}(s)}{Z + D(s)} \right)^* = 0 \quad (11)$$

Letting $s = j\omega$ and expanding equation (11) in a series,

$$1 + \frac{1}{T} \sum_{n=-\infty}^{n=\infty} \frac{N(j\omega + nj\omega_s) G_{ZOH}(j\omega + nj\omega_s)}{Z + D(j\omega + nj\omega_s)} = 0 \quad (12)$$

For $Z = 1$, equation (12) will converge provided the denominator is 1-order higher than the numerator which is the case for most control systems. It is assumed that equation (12) will converge also for different values of Z . This is a reasonable assumption because $|Z| \ll 1.0$ corresponds to a negligible system response; and, in choosing n , one limits the system response given by equation (12) to the significant sidebands of the sampled response.

For the Saturn IB Control system, three terms of equation (12) are generally sufficient for convergence of the series. The 3-term expansion is:

$$1 + \frac{1}{T} \frac{N(j\omega) G_{ZOH}(j\omega)}{Z + D(j\omega)} + \frac{1}{T} \frac{N(j\omega - j\omega_s) G_{ZOH}(j\omega - j\omega_s)}{Z + D(j\omega - j\omega_s)} + \frac{1}{T} \frac{N(j\omega + j\omega_s) G_{ZOH}(j\omega + j\omega_s)}{Z + D(j\omega + j\omega_s)} = 0 \quad (13)$$

For an arbitrary value of frequency ($\omega = \omega_1$) and a given value of sampling frequency ($\omega_s = \omega_{s1}$), equation (13) can be rewritten as,

$$1 + \frac{A_1 + jB_1}{Z + C_1 + jD_1} + \frac{A_2 + jB_2}{Z + C_2 + jD_2} + \frac{A_3 + jB_3}{Z + C_3 + jD_3} = 0 \quad (14)$$

where

$$\begin{aligned} A_1 + jB_1 &= \frac{1}{T} N(j\omega_1) G_{ZOH}(j\omega_1) \\ A_2 + jB_2 &= \frac{1}{T} N(j\omega_1 - j\omega_{s1}) G_{ZOH}(j\omega_1 - j\omega_{s1}) \\ A_3 + jB_3 &= \frac{1}{T} N(j\omega_1 + j\omega_{s1}) G_{ZOH}(j\omega_1 + j\omega_{s1}) \\ C_1 + jD_1 &= D(j\omega_1) \\ C_2 + jD_2 &= D(j\omega_1 - j\omega_{s1}) \\ C_3 + jD_3 &= D(j\omega_1 + j\omega_{s1}) \end{aligned} \quad (15)$$

Equation (14) reduces to a cubic polynomial in Z with complex coefficients. Solving for Z in equation (14) yields three roots: $Z_1(j\omega_1)$, $Z_2(j\omega_1)$, and $Z_3(j\omega_1)$. Combining equations (7) and (10), the result is:

$$\text{OPTVC}(j\omega_1) = -Z_i(j\omega_1) \quad i = 1, 2, 3 \quad (16)$$

Thus, at each value of ω , there are three sets of open-at-TVC phase and gain characteristics. It is not possible to construct a true Nyquist plot from these results because of the multivalued solution of the phase and gain characteristics. A pseudo-Nyquist plot can be constructed by simply plotting all the solutions at each frequency without connecting points. It will be shown in a later section that the multivalued, pseudo-Nyquist plot can be used to interpret the open at TVC stability characteristics of the system in figure 2 in the same manner that a conventional Nyquist plot is employed. Also, the significance of each solution at a given ω will be explained.

An analysis technique for obtaining the frequency response of the system, open at the TVC for a sampled-data control system with discrete and continuous feedback loops, has been developed using the inverse function concept and a series expansion of equation (11). The number of terms required in the series expansion depends on the resonant modes of the system and the sampling rate. If "q" terms are used in the series expansion, then the resultant polynomial from equation (12) will be of the order "q" and there will be "q" open-at-TVC solutions at each ω .

$$\text{OPTVC}(j\omega) = -Z_i(j\omega) \quad i = 1, 2, 3, \dots, q \quad (17)$$

There are no restrictions on the sampling rate provided sufficient terms are taken in equation (12) to obtain the desired range of the continuous system response.

3.0 APPLICATION OF SOLUTION TECHNIQUE TO THE SATURN IB CONTROL SYSTEM IN THE BACKUP GUIDANCE MODE

A method for obtaining a pseudo-Nyquist plot of the open loop gain and phase characteristics at the TVC was developed in section 2.0 for a control system configuration with both sampled-data and continuous feedback control loops. The pseudo-Nyquist plot is a new concept and an example is provided to illustrate the utility of this multivalued polar plot.

3.1 System Description

The Saturn IB first-stage pitch/yaw attitude control system in the backup guidance mode (figure 1) was chosen as an example of a practical control system configuration with both sampled-data and continuous feedback control loops. The planar model of the control system used in this example included the following vehicle degrees of freedom:

- Rigid body rotation
- Rigid body translation
- 5 free-free bending modes

The equations of motion describing the mathematical model of the vehicle and control elements are presented in appendix A. The control system stability characteristics are investigated on a time-invariant (fixed-point) basis. The critical time point chosen for this example ($T = 80$ seconds) is in the maximum aerodynamic pressure region of the trajectory. The vehicle and control system data at 80 seconds of first-stage flight are presented in appendix B. The polynomials used to generate the pseudo-Nyquist plot are also given in appendix B. A sampling period of 0.5 seconds was chosen for this example.

3.2 Interpretation of Pseudo-Nyquist Plot Results

A conventional Nyquist plot for open loop at TVC is presented in figure 3 for the Saturn IB first-stage pitch/yaw control system in the primary guidance mode (continuous system) at $T = 80$ seconds. These typical open-at-TVC results are presented as a baseline comparison for the open-at-TVC pseudo-Nyquist results.

A pseudo-Nyquist plot of the open-at-TVC stability characteristics of the Saturn IB first-stage pitch/yaw attitude control system in the backup guidance mode at $T = 80$ seconds is presented in figure 4. A 3-term expansion of equation (11) was used in generating this plot. The OPTVC (ω) multisolutions are plotted only for the frequency

interval $0 \leq \omega \leq \frac{\omega_s}{2}$, because equation (11) is periodic with ω_s and the plot for the

frequency range from $\frac{\omega_s}{2}$ to ω_s is the mirror image of the plot from 0 to $\frac{\omega_s}{2}$

(reference 6). Note that the plot in figure 4 is comprised of three distinct segments. These three segments represent the multivalued solutions (3 complex roots at each ω) from equation (11). Segment 1 corresponds to the first term, segment 2 to the second term, etc. Furthermore, because the system is continuous at the TVC, each segment represents a portion of the continuous frequency response of the system as measured at the input to the TVC. Note the similarity to figure 3. The multivalued solutions at the reflected frequencies of the first three bending modes are summarized on the figure and noted on the plot by "1" for bending mode 1, etc.

To better illustrate the above points, consider the multivalued solutions from figure 4 which are summarized in table 1. These solutions correspond to the cross-over frequencies for the rigid body gain and phase margins of the system open at TVC.

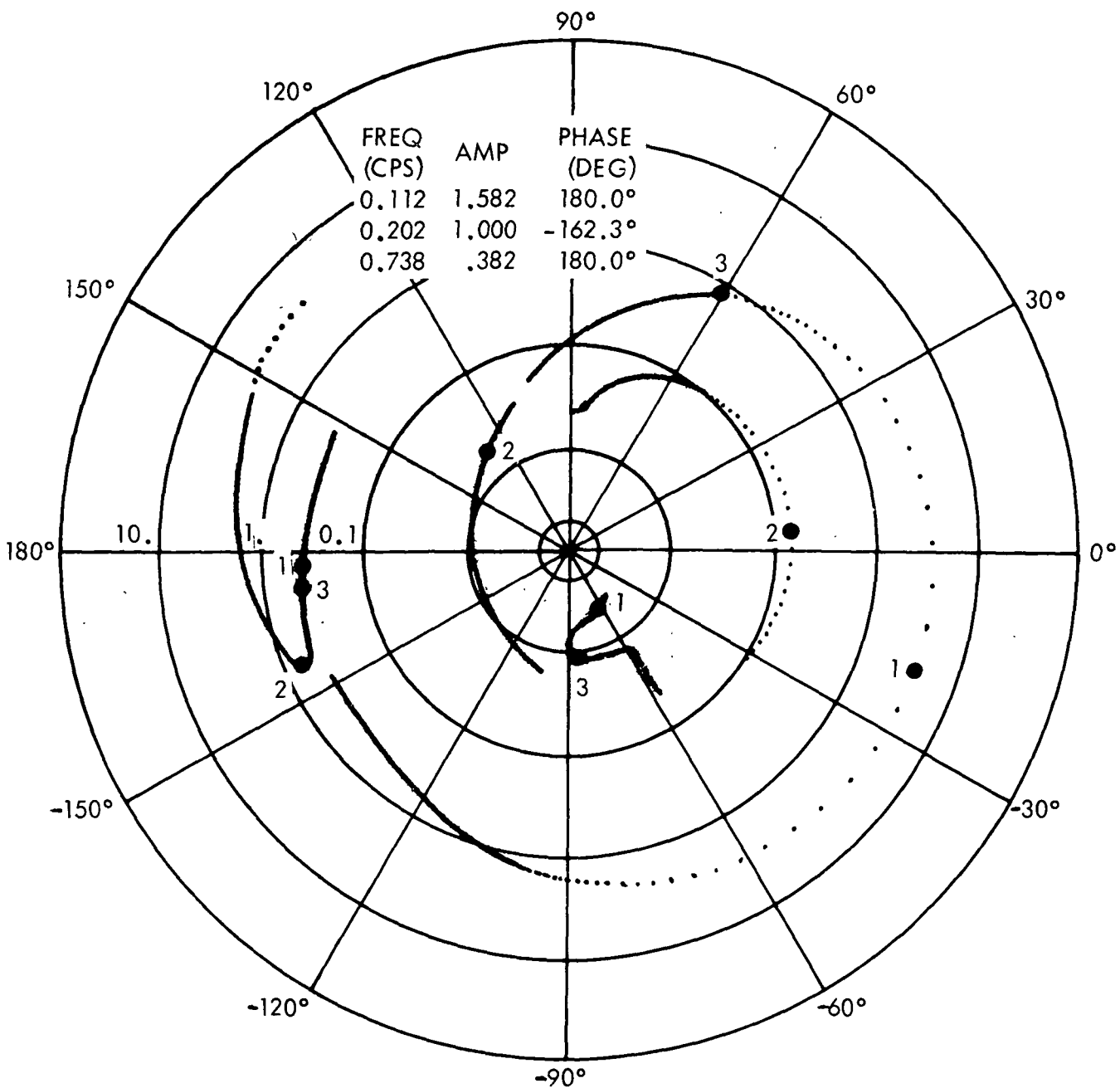
Table 1. Multivalued Solutions at Low Frequency Gain and Phase Margin Crossover Frequencies

Segment	Frequency (Hz)	Amplitude	Phase (Degrees)
1	0.112	1.58200	180.00
2	0.112	0.02567	87.34
3	0.112	0.01197	-120.55
1	0.202	1.00000	-162.29
2	0.202	0.03635	80.90
3	0.202	0.00784	-162.49
1	0.738	0.38200	180.00
2	0.738	0.97134	-108.49
3	0.738	0.00473	-51.06

The results at 0.112 Hz and 0.202 Hz show that two of the multivalued solutions at each of these frequencies are trivial compared to the first value, while the results at 0.738 Hz show that only one of the multivalued solutions is trivial. A better insight into the significance of these results is obtained from a closer examination of the individual terms in the series expansion of equation (11) at the above frequencies.

The components of the 3-term series expansion of equation (11) at 0.112 Hz are:

$$\begin{aligned} \frac{1}{T} N(j\omega) G_{ZOH}(j\omega) &= \frac{1}{T} N(0.112 \text{ Hz}) G_{ZOH}(0.112 \text{ Hz}) = -1.2624 + j 0.56843 \\ D(j\omega) &= D(0.112 \text{ Hz}) = -.31764 - j 0.56368 \\ \frac{1}{T} N(j\omega - j\omega_s) G_{ZOH}(j\omega - j\omega_s) &= \frac{1}{T} N(-1.888 \text{ Hz}) G_{ZOH}(-1.888 \text{ Hz}) = 1.5735E-4 - j2.1068E-3 \end{aligned}$$



FREQ (CPS)	AMP	PHASE (DEG)
0.112	1.582	180.0°
0.202	1.000	-162.3°
0.738	.382	180.0°

MODE	NATURAL FREQ (CPS)	REFLECT FREQ (CPS)	AMP RATIO	PHASE (DEG)	AMP RATIO	PHASE (DEG)	AMP RATIO	PHASE (DEG)
1	1.326	0.674	4.91-03	-64.9	3.96-01	-175.1	3.87+00	-20.3
2	2.327	0.327	2.09-02	124.6	1.55-01	7.7	6.66-01	-156.7
3	2.623	0.623	1.11-02	-89.6	4.17-01	-171.5	7.91-01	62.2

Figure 4. Pseudo-Nyquist Plot for the Saturn IB First-Stage Pitch/Yaw Attitude Control System in the Backup Guidance Mode

$$\begin{aligned}
D(j\omega - j\omega_s) &= D(-1.888 \text{ Hz}) = -6.8786\text{E-}3 - j9.9578\text{E-}3 \\
\frac{1}{T}N(j\omega + j\omega_s)G_{\text{ZOH}}(j\omega + j\omega_s) &= \frac{1}{T}N(2.112 \text{ Hz})G_{\text{ZOH}}(2.112 \text{ Hz}) = -1.1436\text{E-}3 - j1.6516\text{E-}3 \\
D(j\omega + j\omega_s) &= D(2.112 \text{ Hz}) = 8.3727\text{E-}4 + j2.6412\text{E-}2
\end{aligned}
\tag{18}$$

The 3rd-term expansion of equation (11) at 0.112 Hz is:

$$\begin{aligned}
1 + \frac{-1.2624 + j0.56843}{Z - 0.31764 - j0.56368} + \frac{1.5735\text{E-}4 - j2.1068\text{E-}3}{Z - 6.8786\text{E-}3 - j9.9578\text{E-}3} \\
+ \frac{-1.1436\text{E-}3 - j1.6516\text{E-}3}{Z + 8.3727\text{E-}4 + j2.6412\text{E-}2} = 0
\end{aligned}
\tag{19}$$

The first term of equation (19) contains the low-frequency information at 0.112 Hz, the second term of equation (19) reflects the 1.888 Hz system response back to 0.112 Hz, and third term of equation (19) reflects the 2.112 Hz system response back to 0.112 Hz. The triviality of two solutions of equation (19) at 0.112 Hz is attributed to the absence of any significant system resonant modes at 1.888 Hz and 2.112 Hz. This means that variations in the TVC characteristics at these reflected frequencies are not critical. Furthermore, only a one term expansion of equation (11) is necessary to establish the gain margin of the system at 0.112 Hz.

$$1 + \frac{-1.2624 + j0.56843}{Z - 0.31764 - j0.56368} = 0
\tag{20}$$

or

$$Z = 1.58004 - j0.000475 = 1.580/\underline{-0.02^\circ}
\tag{21}$$

from equation (17)

$$\text{OPTVC}(0.112 \text{ Hz}) = -Z = 1.580/\underline{180.02^\circ}
\tag{22}$$

The value of $1.580 / \underline{180.02^\circ}$ using a 1-term expansion of equation (11) compares extremely well with the value of $1.582 / 180.0^\circ$ using a 3-term expansion. This simply means that the other two terms of the expansion contribute very little to refining the solution from the first term. This does not mean that the other two terms are not important at other frequencies, for they still provide information about the open-at-TVC characteristics at the reflected frequencies. At this example frequency, the system response is highly attenuated at 1.888 Hz and 2.112 Hz.

The 0.738-Hz case is a good example where there are two dominant solutions.

The components of the 3-term series expansion from equation (11) at 0.738 Hz are:

$$\begin{aligned}
 \frac{1}{T}N(j\omega) \text{ ZOH}(j\omega) &= \frac{1}{T}N(0.738 \text{ Hz}) \text{ ZOH}(0.738 \text{ Hz}) = 0.052487 + j0.082829 \\
 D(j\omega) &= D(0.738 \text{ Hz}) = 0.45332 - j0.078978 \\
 \frac{1}{T}N(j\omega - j\omega_s) \text{ ZOH}(j\omega - j\omega_s) &= \frac{1}{T}N(-1.262 \text{ Hz}) \text{ ZOH}(-1.262) = 0.16185 + j0.079415 \\
 D(j\omega - j\omega_s) &= D(-1.262 \text{ Hz}) = -0.45119 - j1.0047 \\
 \frac{1}{T}N(j\omega + j\omega_s) \text{ ZOH}(j\omega + j\omega_s) &= \frac{1}{T}N(2.738 \text{ Hz}) \text{ ZOH}(2.738 \text{ Hz}) = 8.8327\text{E-}4 - j1.6449\text{E-}4 \\
 D(j\omega + j\omega_s) &= D(2.738 \text{ Hz}) = 1.7591\text{E-}3 - j3.5474\text{E-}3
 \end{aligned}
 \tag{23}$$

The 3-term expansion of equation (11) at 0.738 Hz is:

$$\begin{aligned}
 1 + \frac{0.052487 + j0.082829}{Z - 0.45332 - j0.078978} + \frac{0.16185 + j0.079415}{Z - 0.45119 - j1.0047} \\
 + \frac{8.8327\text{E-}4 - j1.6449\text{E-}4}{Z + 1.7591\text{E-}3 - j3.5474\text{E-}3} = 0
 \end{aligned}
 \tag{24}$$

In equation (24), the first term contains the low-frequency information at 0.738 Hz, whereas, the second term reflects the 1.262-Hz system response back to 0.738 Hz, and the third term reflects the 2.728-Hz system response back to 0.738 Hz. Again the rigid body gain margin is determined by the first segment or first term of equation (24). In this case, a 1-term expansion would give

$$Z_1 = 0.40083 - j0.003851 = 0.40084 / \underline{-0.55^\circ}
 \tag{25}$$

$$\text{OPTVC}_1(0.738 \text{ Hz}) = -Z_1 = 0.40084 / \underline{179.45^\circ}
 \tag{26}$$

Comparing the value from equation (26) with the 3-term solution for Z_1 in table 1, shows that the other two terms (primarily the second) have a significant effect on the gain margin of the system given by Z_1 . In this case, additional terms are required for proper convergence of Z_1 . The second term of equation (24) folds back information about the system response at 1.262 Hz. The reflected frequency of the second

term is very close to the natural frequency of the first bending mode (1.326 Hz); therefore, the influence of the first bending mode on the system response is given by Z_2 .

As a matter of interest, the reflected responses at the natural frequencies of the first three bending modes used in the example problem are summarized in table 2.

Table 2. Reflected Bending Mode Open-at-TVC Phase and Gain Characteristics

Bending Mode	Natural Frequency (Hz)	Reflected Frequency (Hz)	Segment	Amp Ratio	Phase (Deg.)
1	1.326	.674	2	3.870	-20.3
2	2.327	.327	3	.155	7.7
3	2.623	.623	3	.011	-89.6

The reflected response of the fourth and fifth bending modes (resonant frequencies of 4.924 Hz and 8.532 Hz) are not included in table 2 because additional terms would have been required to obtain their reflected response. A 9-term expansion would be required to obtain the reflected response of the fifth bending mode.

4.0 COMPUTER SIMULATION VERIFICATION OF STABILITY RESULTS

The pseudo-Nyquist plot (figure 4), introduced in section 3.0, was developed to provide a method for determining the stability characteristics of the control system shown in figure 1 in terms of gain and phase variations at the TVC. In this section of the report, it will be shown that the pseudo-Nyquist plot can be used to assess the effect of gain and phase variations at the TVC in the same manner that a conventional Nyquist plot is used. This will be accomplished by correlating the stability results from the pseudo-Nyquist plot in figure 4 with the results from a fixed-point digital computer simulation of the vehicle time response at 80 seconds of first-stage flight. The mathematical model and input data used in the digital simulation are identical to those used in section 3.0. The rigid body gain margins at 0.112 Hz and 0.738 Hz will be verified using the time response results from a computer simulation to show that the pseudo-Nyquist plot yields the correct low-frequency stability margins. The gain and phase characteristics of the first and second bending modes in figure 4 will also be verified using the digital simulation.

4.1 Verification of Rigid Body Stability Margins

The low-frequency gain margins at 0.112 Hz and 0.738 Hz mean that if the gain at the TVC (K) were reduced by a factor of 1.0/1.582 or increased by a factor of 1.0/0.382, respectively, the system would be neutrally stable. To verify these gain margins, system time responses were obtained for cases where K was decreased by a factor of 1.0/1.582 \pm 5% and increased by a factor 1.0/0.382 \pm 5%. Because a reduction in actuator gain by a factor of 1.0/1.582 causes a neutrally stable condition, the \pm 5% variations will show the stable and unstable conditions which exist on either side of the neutral stability point.

Figure 5 shows the engine gimbal angle time histories for these gain variations. These results confirm the vehicle low-frequency stability characteristics predicted by the pseudo-Nyquist plot in figure 4.

4.2 Verification of Bending Mode Stability Characteristics

To verify that the pseudo-Nyquist plot gives the correct open-at-TVC bending stability characteristics for the backup guidance system, the following approach was taken. In figure 4, the segment that contains the first bending mode resonant response crosses the 0.0-degree axis with a magnitude of 3.5, and the segment that contains the second bending mode resonant response crosses the 0.0-degree axis with a magnitude of 0.151. If the gain of the first bending mode response could be decreased by a factor of 3.5, and the phase of the first bending mode response changed by 180 degrees, the first bending mode response should cross the 180-degree axis with an amplitude of 1.0. Likewise, if the gain of the second bending mode response could be increased by a factor of 1/0.151, and the phase of the second bending mode response changed by 180 degrees, the second bending mode response should cross the 180-degree axis with an amplitude of 1.0. It is well known that the resonant gain of a bending mode is inversely proportional to its generalized mass. Furthermore,

$$\text{OPTVC}(\omega = \omega_{B_i}) \sim \frac{1}{M_{B_i}} \quad (27)$$

The generalized mass of the first and second modes can be manipulated to achieve a neutral stability condition which can easily be checked by simulation results.

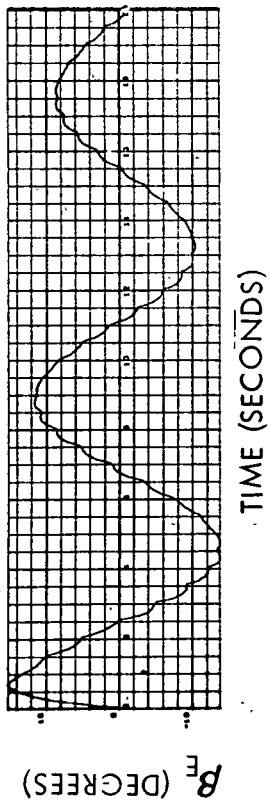
The new pseudo-Nyquist plots generated using the modified generalized masses are presented in figures 6 and 7. Figure 6 shows the results for the case where first bending mode generalized mass is multiplied by -3.5, and figure 7 shows the results for the case where the second mode generalized mass is multiplied by -0.151. Figures 6 and 7 show that the individual responses of each bending mode cross the 180-degree axis very close to the -1.0 point. The response of the two bending modes does not cross exactly at the -1.0 point because of the approximate nature of the relationship given by equation (27). Changing the generalized mass of a given bending mode also changes the coupled response given by the denominator of equation (4). For large changes in generalized mass, gross changes in the system response can result as illustrated by the low-frequency segment of figure 7.

The results of figures 6 and 7 show that the responses of the two bending modes cross the 180-degree axis at a gain of about 1.15. The generalized masses of the two modes were adjusted by a factor of 1.15 and simulation time responses were obtained. The results are shown in figures 8 and 9. Case 1 (figure 8) shows the time response results for a first mode generalized mass multiplied by -3.5 (1.15). The first bending mode response is shown to be neutrally stable for a step attitude command of one degree. Likewise, the second bending mode response is very close to neutral stability in Case 2 (figure 9) where the generalized mass of that mode was changed by -0.151 (1.15).

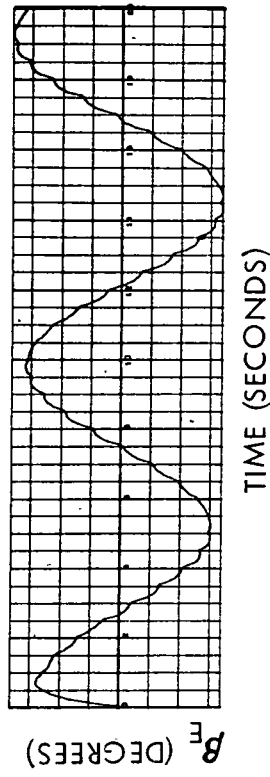
The results presented in this section confirm that the pseudo-Nyquist plot can be used to predict the continuous open-at-TVC stability margins of a control system containing both discrete and continuous feedback loops.

GAIN MARGIN AT $\omega = 0.112\text{HZ}$

$K = 1.05 (1.0/1.582)$

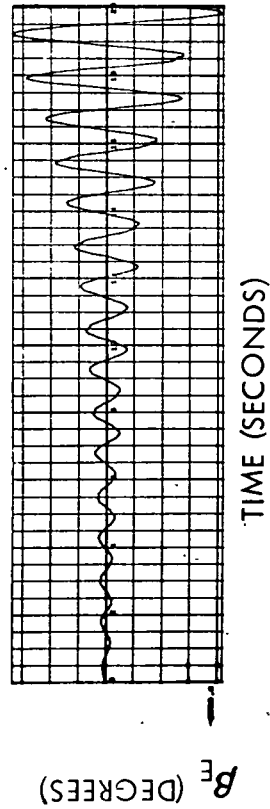


$K = .95 (1.0/1.582)$



GAIN MARGIN AT $\omega = 0.738\text{HZ}$

$K = 1.05 (1.0/.382)$



$K = .95 (1.0/.382)$

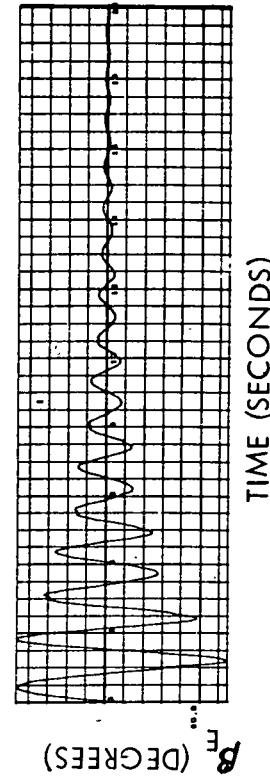
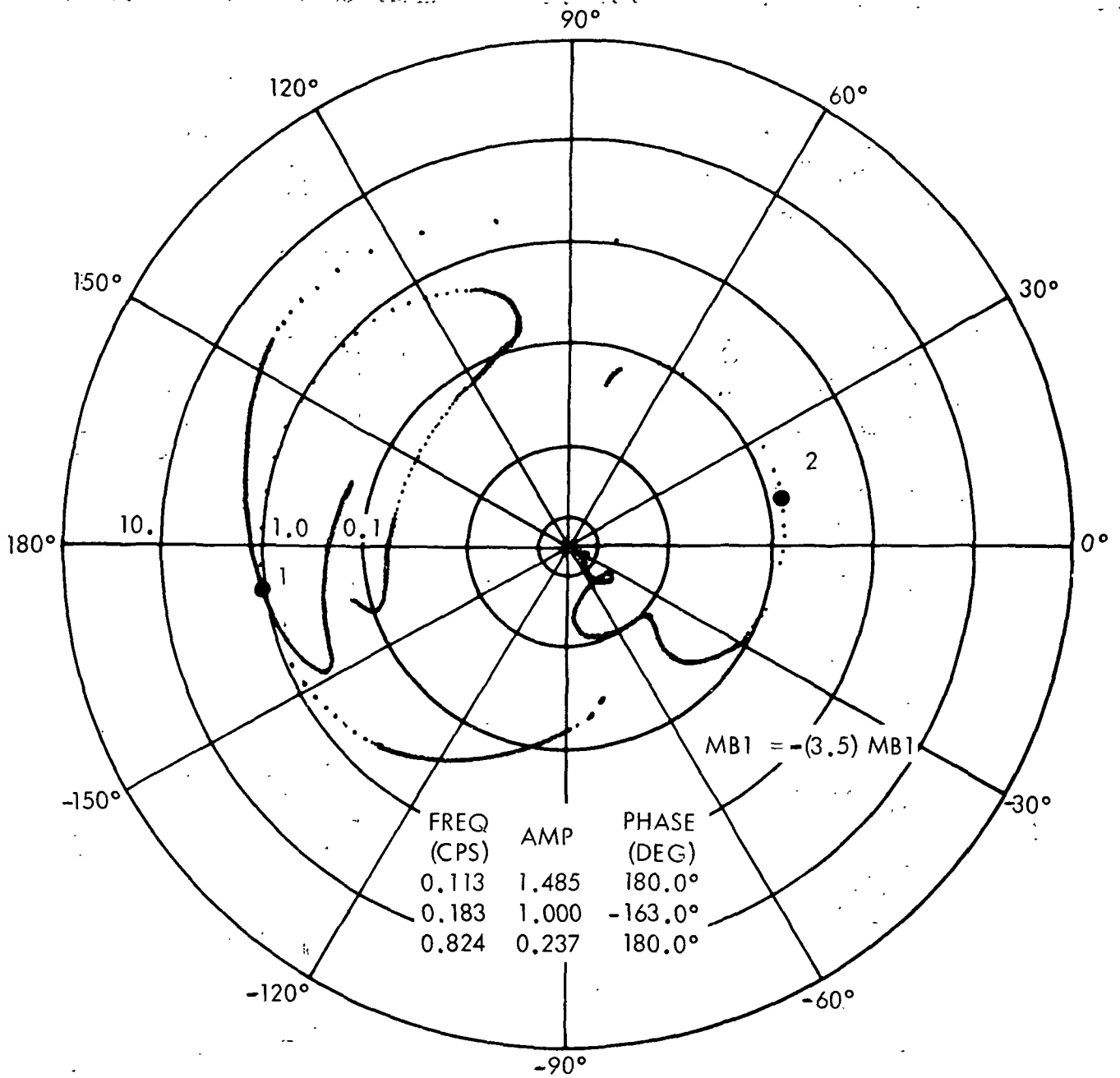
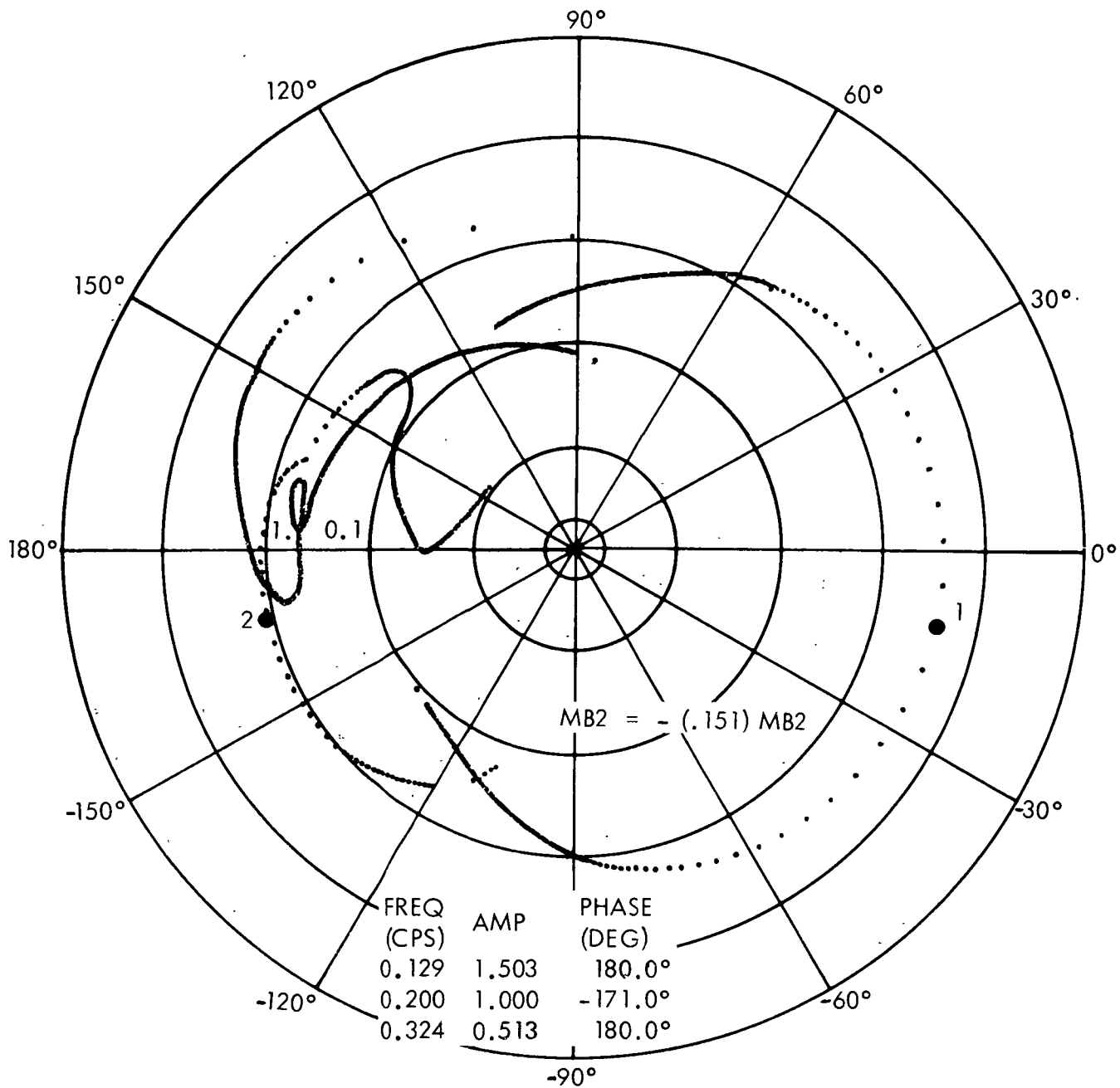


Figure 5. Confirmation of Low-Frequency Gain Margins from Pseudo-Nyquist Plot



MODE	NATURAL FREQ (CPS)	REFLECT FREQ (CPS)	AMP RATIO	PHASE (DEG)	AMP RATIO	PHASE (DEG)	AMP RATIO	PHASE (DEG)
1	1.326	0.674	3.78-03	-40.3	3.01-01	-166.5	1.16+00	170.9
2	2.327	0.327	8.82-02	-89.2	1.60-01	8.1	5.94-01	-151.2

Figure 6. Pseudo-Nyquist Plot Using Modified First Bending Generalized Mass

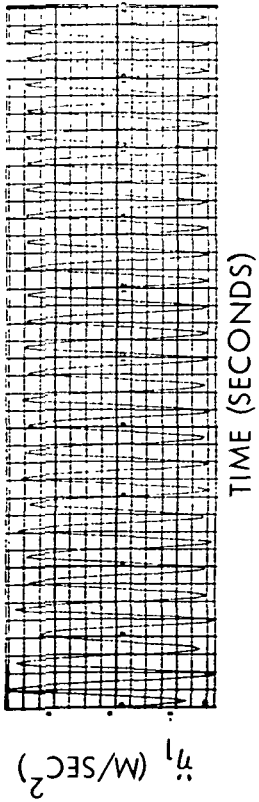


FREQ (CPS)	AMP	PHASE (DEG)
0.129	1.503	180.0°
0.200	1.000	-171.0°
0.324	0.513	180.0°

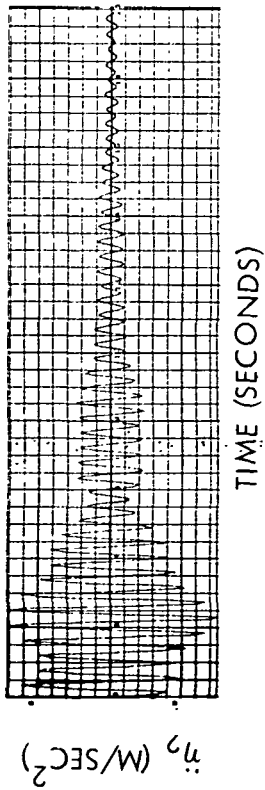
MODE	NATURAL FREQ (CPS)	REFLECT FREQ (CPS)	AMP RATIO	PHASE (DEG)	AMP RATIO	PHASE (DEG)	AMP RATIO	PHASE (DEG)
1	1.326	0.674	6.94-02	162.7	2.06-01	134.5	3.93+00	-19.6
2	2.327	0.327	2.92-01	95.5	5.11-01	179.2	1.26+00	-165.8

Figure 7. Pseudo-Nyquist Plot Using Modified Second Bending Generalized Mass

$$M_{\beta 1} = - (3.5)(1.15) MB1$$



$$M_{\beta 1} = - (3.5)(1.15) MB1$$



$$M_{\beta 1} = - (3.5)(1.15) MB1$$

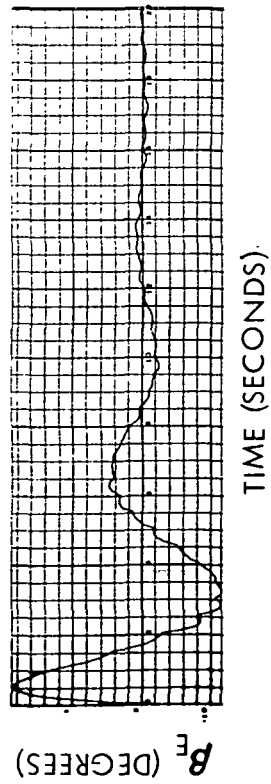
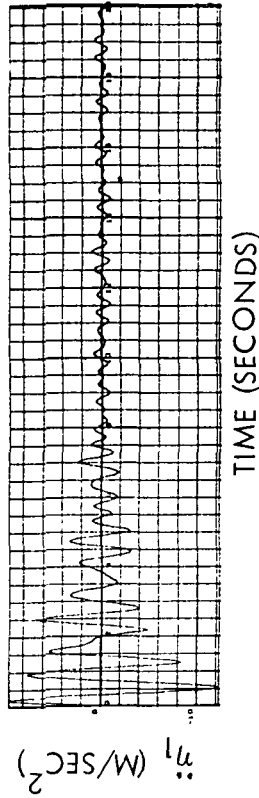
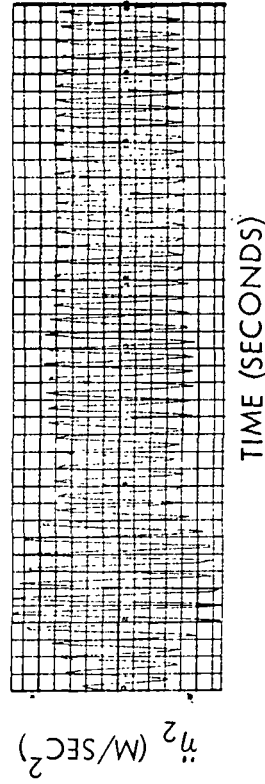


Figure 8. Confirmation of First Bending Mode Stability Margins from Pseudo-Nyquist Plot

$$M_{\beta 2} = - (.151)(1.15) MB2$$



$$M_{\beta 2} = - (.151)(1.15) MB2$$



$$M_{\beta 2} = - (.151)(1.15) MB2$$

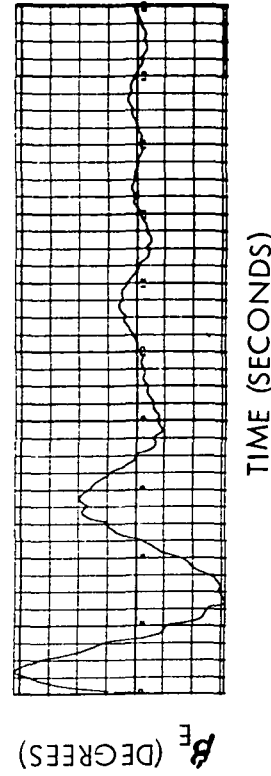


Figure 9. Confirmation of Second Bending Mode Stability Margins from Pseudo-Nyquist Plot

CONCLUDING REMARKS

A solution technique has been developed for obtaining the frequency response characteristics at the input to the TVC (a continuous element) of an attitude control system with both sampled-data and continuous feedback loops. The inverse function concept is used in conjunction with a series expansion of the pulse-transform of the characteristic equation of the system to obtain an explicit solution for the open-at-TVC response. The solution technique is essentially the universal problem of solving for the roots of an n-order polynomial with complex coefficients at various frequencies over the frequency interval from 0 to $\frac{\omega_s}{2}$. The order of the polynomial (n) is equal to the number of terms of the series expansion. The series must be convergent which it is for control systems with low band-pass characteristics. The number of terms required depends on the resonant modes of the system (i. e. eigenvalues) and the sampling frequency.

The multivalued solutions from this new technique can be plotted as a pseudo-Nyquist plot. The pseudo-Nyquist plot can be utilized in the same manner as a conventional Nyquist plot to determine the system stability characteristics of a sampled-data control system with single rate sampled-data and continuous feedback loops.

APPENDIX A

This appendix presents the equations of motion used in the analyses presented in this report. Figure A-1 shows the coordinate system associated with the equations of motion.

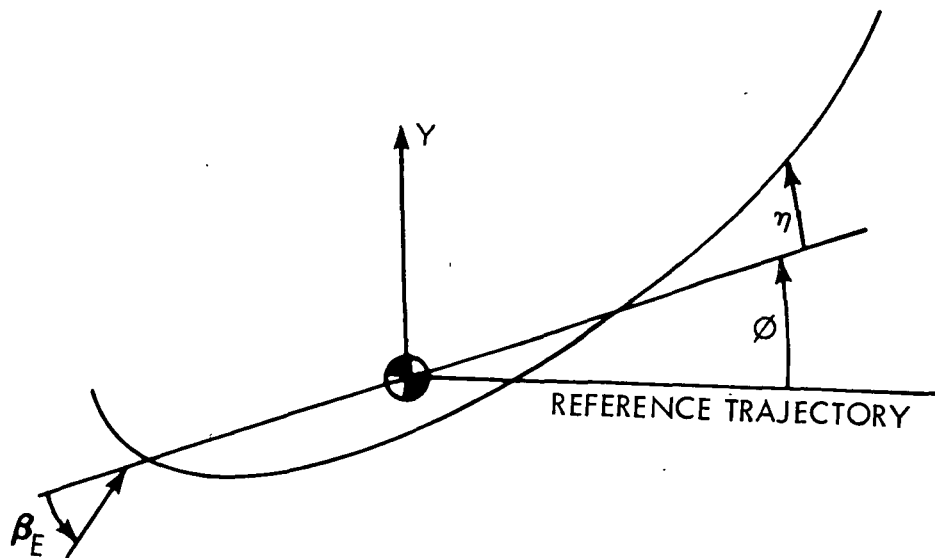


Figure A-1. Coordinate System for Equations of Motion

Rigid Body Rotation Equation (ϕ)

$$I \ddot{\phi} + C_{n\alpha} q A_R (X_E - X_{cp}) \phi - \frac{C_{n\alpha} q A_R (X_E - X_{cp})}{V} \dot{Y}$$

$$- \sum_{i=1}^5 (F - X) (X_E Y_i'(X_E) - Y_i(X_E)) \eta_i + F_G X_E \beta_E = 0$$

Rigid Body Translation Perpendicular to Trajectory (Y)

$$M \ddot{Y} + \frac{C_{n\alpha} q A_R}{V} \dot{Y} - (\bar{g} M + C_{n\alpha} q A_R) \phi$$

$$+ \sum_{i=1}^5 (F - X) Y_i'(X_E) \eta_i - F_G \beta_E = 0$$

Bending Degrees of Freedom (η_i , $i = 1, 2, 3, 4, 5$)

$$M_{Bi} \ddot{\eta}_i + 2 \zeta_{Bi} \omega_{Bi} M_{Bi} \dot{\eta}_i + \omega_{Bi}^2 M_{Bi} \eta_i$$

$$- (S_E Y_i(X_E) + \theta_E Y_i'(X_E)) \ddot{\beta}_E - F_G Y_i(X_E) \beta_E = 0$$

Sensed Attitude at the Platform (ϕ_s)

$$\phi_s = \phi - \sum_{i=1}^5 Y_i'(PG) \eta_i$$

Sensed Attitude Rate at the Rate Gyro Location ($\dot{\phi}_s$)

$$\dot{\phi}_s = \dot{\phi} - \sum_{i=1}^5 Y_i'(RG) \dot{\eta}_i$$

Sensed Acceleration at the Accelerometer Location (\ddot{y}_s)

$$\begin{aligned} \ddot{y}_s &= \ddot{Y} - \bar{X}_A \ddot{\phi} - \bar{g} \phi + \sum_{i=1}^5 Y_i(A) \ddot{\eta}_i \\ &+ \sum_{i=1}^5 \bar{g} Y_i'(A) \eta_i = 0 \end{aligned}$$

Control Equation (β_E)

$$\beta_E = G_{TVC}(s) \left\{ a_0 F_{\phi}(s) (\phi_s - \phi_c) + a_1 F_{\dot{\phi}}(s) \dot{\phi}_s + g_2 F_{\ddot{y}}(s) \ddot{y}_s \right\}$$

APPENDIX B

This appendix presents the data used in the analyses presented in this report. These data are typical Saturn IB vehicle and Control System data.

T	= 80.0 seconds	M	= 356571.0 kg
F	= 8231172.0 Newtons	F _G	= 4115586.0 Newtons
X	= 474030.0 Newtons	\bar{g}	= 21.756 m/sec ²
q	= 32278.0 Newtons/m ²	V	= 546.5 m/sec
I	= 73671632.0 kg-m ²	\bar{X}_E	= 17.25 m
X _{cp}	= 28.07 m	C _{nα}	= 5.18 per rad
\bar{X}_A	= -22.91 (m)	A _R	= 33.468 m ²
a _o	= 1.85 deg per deg	a ₁	= 1.65 deg per deg/sec
g ₂	= 4.0 deg per m/sec ²		

Saturn IB First-Stage Pitch/Yaw Bending Data at T = 80 Seconds

MODE	FREQUENCY (RAD/SEC)	FREQUENCY (CPS)	SLOPE AT IU PLATFORM (PER M)	SLOPE AT RATE GYRO (PER M)	DISPLACEMENT AT ACCELEROMETER
1	8.322+00	1.326+00	-1.249-02	-1.249-02	1.130-02
2	1.462+01	2.327+00	1.479-02	1.479-02	-1.064-01
3	1.648+01	2.623+00	6.600-03	6.600-03	-2.258-02
4	3.094+01	4.925+00	1.788-02	1.788-02	1.205-01
5	5.361+01	8.532+00	2.602-02	2.602-02	4.722-01

MODE	FREQUENCY (RAD/SEC)	FREQUENCY (CPS)	GENERALIZED MASS (KG)	DEFLECTION AT GIMBAL	SLOPE AT GIMBAL (PER M)
1	8.332+00	1.326+00	4.455+03	8.287-02	5.467-03
2	1.462+01	2.327+00	2.780+03	-3.932-02	-1.698-03
3	1.648+01	2.623+00	2.682+04	6.151-02	-3.213-03
4	3.094+01	4.925+00	3.982+04	5.316-01	8.820-02
5	5.361+01	8.532+00	3.195+04	-1.046-02	-6.450-02

MODE	FREQUENCY (RAD/SEC)	FREQUENCY (CPS)	SLOPE AT S/C PLATFORM (PER M)
1	8.332+00	1.326+00	-3.437-2
2	1.462+01	2.327+00	-3.132-2
3	1.648+01	2.623+00	-7.491-3
4	3.094+01	4.925+00	8.260-3
5	5.361+01	8.532+00	3.886-2

Control Filter and Actuator Data:

$$G_{TVC}(s) = \frac{1.0}{9.293E-13 s^6 + 5.773E-10 s^5 + 1.669E-7 s^4 + 2.685E-5 s^3 + 1.232E-3 s^2 + 6.308E-2 s + 1.0}$$

$$F_{\phi}(s) = \frac{1.0}{0.17 s + 1.0}$$

$$F_{\dot{\phi}}(s) = \frac{0.0035 s^2 + 0.01 s + 1.0}{0.001679 s^3 + 0.028568 s^2 + 0.24518 s + 1.0}$$

$$F_{\ddot{\phi}}(s) = \frac{1.0}{0.5 s^2 + 5.1 s + 1.0}$$

REFERENCES

1. Holzman, J.; Neumann, J. W.; Rockey, R. J.; Van Calcar, H. and Wakamiya, Y.: Digital Control System Design For Saturn Class Vehicles. TRW Report 4185-6014-RU000, April 16, 1965.
2. Phillips, C. L.: Digital Compensation of the Thrust Vector Control System. Auburn University, September 28, 1965.
3. Maggiore, J. J.: Stability Analysis of AAP-2 Launch Vehicle With Backup Guidance System. CCSD Technical Note TN-AP-70-446, March 6, 1970.
4. Burnitt, M. G; Davis, C. W. and Gordo, M.: Investigation of Proposed Spacecraft Software Changes in the Saturn IB/Skylab Backup Guidance System. CCSD Technical Note TN-AP-71-520, July 1971.
5. Davis, C. W.: SL-2/S-IB Stage Backup Guidance System Stability Margin Assessment. CCSD Technical Note TN-AP-72-536, February 1972.
6. Kuo, Benjamin C.: Analysis and Synthesis of Sampled-Data Control Systems. Prentice - Hall Inc., 1963.



POSTMASTER: If Undeliverable (Section 158
Postal Manual) Do Not Return

"The aeronautical and space activities of the United States shall be conducted so as to contribute . . . to the expansion of human knowledge of phenomena in the atmosphere and space. The Administration shall provide for the widest practicable and appropriate dissemination of information concerning its activities and the results thereof."

—NATIONAL AERONAUTICS AND SPACE ACT OF 1958

NASA SCIENTIFIC AND TECHNICAL PUBLICATIONS

TECHNICAL REPORTS: Scientific and technical information considered important, complete, and a lasting contribution to existing knowledge.

TECHNICAL NOTES: Information less broad in scope but nevertheless of importance as a contribution to existing knowledge.

TECHNICAL MEMORANDUMS: Information receiving limited distribution because of preliminary data, security classification, or other reasons. Also includes conference proceedings with either limited or unlimited distribution.

CONTRACTOR REPORTS: Scientific and technical information generated under a NASA contract or grant and considered an important contribution to existing knowledge.

TECHNICAL TRANSLATIONS: Information published in a foreign language considered to merit NASA distribution in English.

SPECIAL PUBLICATIONS: Information derived from or of value to NASA activities. Publications include final reports of major projects, monographs, data compilations, handbooks, sourcebooks, and special bibliographies.

TECHNOLOGY UTILIZATION PUBLICATIONS: Information on technology used by NASA that may be of particular interest in commercial and other non-aerospace applications. Publications include Tech Briefs, Technology Utilization Reports and Technology Surveys.

Details on the availability of these publications may be obtained from:

SCIENTIFIC AND TECHNICAL INFORMATION OFFICE

NATIONAL AERONAUTICS AND SPACE ADMINISTRATION
Washington, D.C. 20546